Towards the identification of the binding site of benzimidazoles to β-tubulin of *Trichinella spiralis*: Insights from computational and experimental data

Rodrigo Aguayo-Ortiz[a], Oscar Méndez-Lucio[a], José L. Medina-Franco[b], Rafael Castillo[a], Lilián Yépez-Mulia[c], Francisco Hernández-Luis[a], Alicia Hernández-Campos[a,*]

[a] *Facultad de Química, Departamento de Farmacia, Universidad Nacional Autónoma de México, México, DF 04510, Mexico*
[b] *Instituto de Química, Universidad Nacional Autónoma de México, México, DF 04510, Mexico*
[c] *Unidad de Investigación Médica en Enfermedades Infecciosas y Parasitarias, IMSS, México, DF 06720, Mexico*

ARTICLE INFO

ABSTRACT

Benzimidazole-2-carbamate derivatives (BzC) are among the most important broad-spectrum anthelmintic drugs for the treatment of nematode infections. BzC selectively bind to the β-tubulin monomer and inhibit microtubule polymerization. However, the crystallographic structure of the nematode tubulin and the mechanism of action are still unknown. Moreover, the relation between the mechanism of action and the binding site of BzC has not yet been explained accurately. By using the amino acid sequence of *Trichinella spiralis* β-tubulin as a basis and by applying homology modeling techniques, we were able to build a 3D structure of this protein. In order to identify a binding site for BzC, molecular docking and molecular dynamics calculations were carried out with this model. The results were in good agreement with the most common amino acid mutations associated with drug resistance (F167Y, E198A and F200Y) and with the experimental results of competitive inhibition of colchicine binding to tubulin. Besides, Glu198, Thr165, Cys239 and Gln134 were identified as important amino acids in the binding process since they directly interact with BzC in the formation of hydrogen bonds. The results presented in this paper are a step further towards the understanding, at the molecular level, of the mode of action of anthelmintic drugs. These results constitute valuable information for the design or improvement of more potent and selective molecules.

© 2013 Elsevier Inc. All rights reserved.

1. Introduction

The parasitic infection caused by the intestinal nematode *Trichinella spiralis* (trichinellosis) is one of the most important neglected tropical diseases (NTDs) [1]. This infection has been treated with a number of current broad-spectrum anthelmintic drugs, many of which act by means of the inhibition of microtubule polymerization, interrupting the growth of the parasite. The polymerization and depolymerization of microtubules is accomplished by the stability and solubility of the α/β-tubulin heterodimer, which is the basic unit of microtubules [2,3].

Benzimidazole-2-carbamate derivatives (BzC) are among the most widely used antinematodal drugs; they also show high efficacy against trematodes, cestodes and some protozoa parasites [3–5]. Carbendazim (CBZ, methyl 1*H*-benzimidazole-2-ylcarbamate) derivatives are the representative compounds of this group, among which the most commonly used as antiparasitic agents are the 5(6)-substituted benzimidazole-2-carbamates.

These BzC include important drugs such as albendazole (ABZ), fenbendazole (FBZ), mebendazole (MBZ), nocodazole (NZ), oxibendazole (OBZ), parbendazole (PBZ), luxabendazole (LBZ) and the sulfoxide metabolites of ABZ (ABZSO, ricobendazole) and FBZ (FBZSO, oxfendazole) [6]. Several studies have shown that the mode of action of these BzC is the inhibition of microtubule polymerization by selectively binding to the β-tubulin monomer of the parasite, but having little effect due to binding tubulin of the mammalian host [7,8]. This mode of action has been demonstrated by ultrastructural studies and the sequence analysis of resistant organisms, indicating that BzC normally present a high affinity for the region located between the N-terminal domain (residues 1–201) and the intermediate domain (202–371) [4,7,9–11]. Similar observations have been made for other helminths, fungi and protozoa.

Despite the information available of the parasitic β-tubulin, the lack of a crystallographic structure has hampered the identification of the binding site of BzC. However, the increasing diversity of structural templates has led to the generation of more accurate three-dimensional (3D) structures using homology modeling. This structure prediction technique establishes that a folding of a protein is more evolutionarily conserved than its amino acid sequence, thus confirming, by methodological information, that homology

modeling is suitable for use in molecular docking studies in the absence of crystallographic structures [12,13].

Experimental reports have identified single amino acid mutations associated with the loss of BzC-β-tubulin affinity as the major causes of drug resistance. The most common mutations are F167Y, E198A and F200Y [14], which have been observed in several nematodes such as *Haemonchus contortus* [2,15–17], *Teladorsagia circumcincta* [18], *Trichuris trichiura* [19], *Wuchereria bancrofti* [20], among others. Several authors have proposed binding-site models, using homology modeling; these give rise to different possible explanations of the binding modes based on experimental results [21–24].

In addition to BzC, colchicine is one of the most important microtubule inhibitors. This molecule promotes microtubule depolymerization by binding to a single high-affinity site on the β-tubulin subunit near the monomer-monomer interface in the unpolymerised α/β-tubulin dimer [3]. Interestingly, competitive inhibition studies on mammalian isolated tubulins show that colchicine and BzC bind to the same pocket near the N-terminal domain [8,25–28]. Preliminary computational studies using pharmacophore modeling, conducted with a few BzC, support the possible binding on the colchicine-binding site. However, more experimental evidence is required to confirm this hypothesis [29].

Notwithstanding the experimental information concerning the resistance mutations, the mechanism of action and the competitive inhibition with colchicine, there is currently no record of a binding site model that can explain all three of them [21–24]. In this paper, we propose a binding pocket and binding mode for BzC in β-tubulin by carrying out a comprehensive computational study applying homology modeling, molecular docking and molecular dynamics simulations. The results suggest a binding pocket and a binding mode which are in agreement with the experimental information mentioned above.

2. Materials and methods

2.1. Template and binding-site identification

The amino acid sequence of *T. spiralis* β-tubulin (GenBank: EFV50889) was retrieved from the NCBI GenBank database [30] on the FASTA format. This sequence was submitted to a template and binding site identification using the I-TASSER server (http://zhanglab.ccmb.med.umich.edu/I-TASSER/) [31]. The D chain, which is present in the β-subunit of the heterotetrameric structure of *Ovis aries* (PDB ID: 3N2G_D) [32], was chosen as a template based on the presence of amino acids associated with nematode resistance in the binding site found by I-TASSER.

2.2. β-Tubulin homology modeling

The homology modeling process was carried out with MODELLER 9v10 software [33], using residues 1–428 of the *T. spiralis* β-tubulin sequence. The resulting model was evaluated by the QMEAN6 score to obtain an estimation of the local model quality, whereas the quality of the protein stereochemistry was assessed using PROCHECK [34]. The model was subjected to energy minimization employing the GROMOS96 43a1 force field, a single point charge water model with a time step of 0.002 ps, using GROMACS 4.5.3 software [35].

2.3. Molecular docking studies

The compounds in Table 1 were subjected to molecular docking with the homology model of *T. spiralis* β-tubulin. The goal was to help rationalize, at the molecular level, the importance of the structural features in BzC derivatives and their implication in ligand–protein interaction. All the BzC shown in Table 1 were submitted to a geometry optimization using the MMFF94x force field. The torsional root and branches of the ligands were chosen utilizing MGLTools 1.5.4 [36], allowing flexibility for all rotatable bonds of the ligand except for the amide bond, which was fixed. In addition, MGLTools 1.5.4 was used to assign Gasteiger–Marsilli atomic charges to all ligands. It is important to mention that the isomerism of the carbamate group and the inherent tautomerism to the benzimidazole ring system were also taken into account. This considerations led to four different groups of molecules: *cis*-1,5; *trans*-1,5; *cis*-1,6 and *trans*-1,6 (Table 1). The enantiomeric behavior of ABZSO and FBZSO was also taken into account.

Docking calculations were performed with AutoDock 4.2 software [36]. A three-dimensional grid box of size 80 Å × 80 Å × 80 Å, with 0.375 Å spacing and centered at the amino acid Phe200, whose mutation is associated with resistance (see below), was calculated for the following atom types: H, HD, C, A, N, NA, OA, F, P, S, SA, Cl, Br, and I. In this paper, the conformational search of the ligand was carried out using a Lamarckian genetic algorithm. A total of 20 runs were undertaken with a maximal number of 5,000,000 energy evaluations and initial populations of 150 conformers. The best binding mode of each molecule present in the four groups was selected based on the lowest free binding energy.

2.4. Molecular dynamics simulations

Two molecular dynamics (MD) of *T. spiralis* β-tubulin, with and without a ligand, were performed using GROMACS 4.5.3 software. The initial structures of the two simulations were the results from the homology model and the ligand-protein complexes with the lowest binding energy, respectively. The ligand parameters were calculated with PRODRG server [37] in the framework of the GROMOS force field. The protein and the complexes were solvated with water in a periodic cubic box that comprised the protein and 1.0 nm of water on all sides. Na+ and Cl− atoms were added randomly in order to neutralize the charge of the system and to achieve a concentration of 0.15 M. All the simulations were carried out at 1 bar and 300 K.
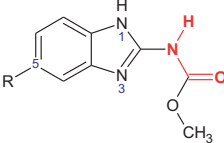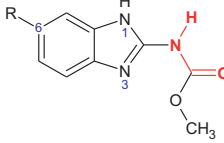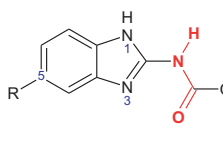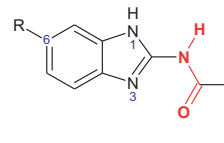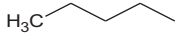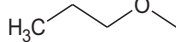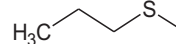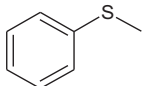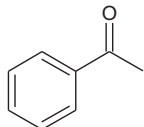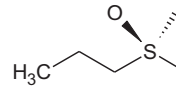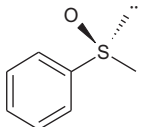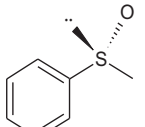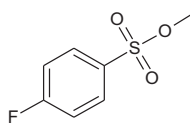
First, an energy minimization of the system was carried out employing the GROMOS96 43a1 force field [38], a single point charge water model and a time step of 0.002 ps. Electrostatic forces were calculated with the PME implementation of the Ewald summation method [39], and the Lennard-Jones and Coulomb interactions were computed within a cut-off radius of 1.0 nm. Following energy minimization, the system was equilibrated by 20 ps of MD with position restraints on the protein, enabling the relaxation of the solvent molecules. Finally, a 10 ns MD was performed on the β-tubulin model and 3 ns for each of the ligands in the complexes to equilibrate the corresponding systems.

RMSD, hydrogen bonding and binding free energy of the complex were analyzed during the molecular dynamics study. The calculation of the binding free energy was based on the linear interaction energy (LIE) method equation:

$$\Delta G_{\text{bind}} = \alpha[(V_{\text{LJ}})_{\text{bound}} - (V_{\text{LJ}})_{\text{free}}] + \beta[(V_{\text{CL}})_{\text{bound}} - (V_{\text{CL}})_{\text{free}}] + \gamma \quad (1)$$

where $(V_{\text{LJ}})_{\text{bound}}$ is the average Lennard-Jones energy for ligand–protein interaction; $(V_{\text{LJ}})_{\text{free}}$ is the average Lennard-Jones energy for l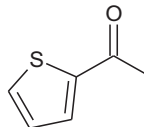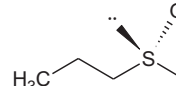igand–water interaction; $(V_{\text{CL}})_{\text{bound}}$ is the average electrostatic energy for ligand–protein interaction; $(V_{\text{CL}})_{\text{free}}$ is the average electrostatic energy for ligand–water interaction; α, β and γ are the LIE coefficients. For small drug-like ligands $\alpha = 0.18$, $\beta = 0.50$ and $\gamma = 0.00$ [40,41].

Table 1
Chemical structures of the BzC microtubule inhibitors.

cis-1,5 **cis-1,6** **trans-1,5** **trans-1,6**

Compound	R	Compound	R	Compound	R
CBZ (carbendazim)	H	PBZ (parbendazole)	H₃C〜〜	OBZ (oxibendazole)	H₃C〜〜O〜
ABZ (albendazole)	H₃C〜〜S〜	FBZ (fenbendazole)	〜S〜	MBZ (mebendazole)	〜C(=O)〜
(+) ABZSO (ricobendazole)	H₃C〜〜S(=O)〜	(+) FBZSO (oxfendazole)	〜S(=O)〜	NZ (nocodazole)	〜S〜C(=O)〜
(−) ABZSO (ricobendazole)	H₃C〜〜S(=O)〜	(−) FBZSO (oxfendazole)	〜S(=O)〜	LBZ (luxabendazole)	F〜〜S(=O)₂O〜

3. Results and discussion

3.1. Homology modeling and binding site prediction

Since at present time the crystallographic structure of β-tubulin from *T. spiralis* is not available, we had to generate a homology model by searching for a template based on the record of resistance mutations present in helminths. There are reports of amino acid mutations in the β-tubulin monomer that lead to the resistance of helminths, for example: Phe167 [42], Glu198 [15,16] and Phe200 [17,18]. Based on these amino acids, the template protein was selected, employing the Predicted Binding Site module of I-TASSER [31], which was used to generate a homology model of β-tubulin. As a result of this search, we were able to identify two possible templates, one of which was the model created by M.K. Robinson (PDB ID: 1OJ0_A) [21], whereas the second belongs to a β-tubulin of *O. aries* (PDB ID: 3N2G_D) [32]. An interesting aspect of the latter template is that the co-crystallized ligand ID: G2N (chemical structure shown in Fig. S1 of the Supplementary data), located at the binding site presents a carbamate group in its structure. The molecular similarity between the co-crystallized ligand of PDB ID: 3N2G_D and BzC suggests a related binding mode for these antiparasitic molecules. In this study, the *O. aries* β-tubulin (PDB ID: 3N2G_D) was chosen as a template to generate the structure of *T. spiralis* tubulin.

The alignment of the template and the target sequences showed a 94.86% of identity, with 406 identical positions and 18 similar positions (Fig. 1). MODELLER 9v10 software was used to generate a 3D model of the *T. spiralis* β-tubulin using PDB ID: 3N2G_D as a template. The model was minimized using the GROMACS 4.5.3 software with the conditions previously described (see Section 2). The analysis of the Ramachandran plot (Fig. S2 in the Supplementary data), generated with the program PROCHECK [34], indicates a reliability of 96.7%, and it locates all the amino acids corresponding to the binding site of the co-crystallized ligand in the allowed

regions. The PROCHECK server also showed an acceptable global Z-score value (−1.77) and a QMEANscore [43] of 0.62, a value slightly lower than the limit of two standard deviations, but still acceptable for a large protein structure (Fig. S2 in the Supplementary data). Indeed the quality of this model makes it appropriate for molecular docking studies.

The identified binding pocket is comprised of the amino acids Phe167, Glu198 and Phe200, which are among the most important amino acids associated with the resistance of helminths (Fig. 2). The proposed binding site in the β-tubulin model is located near the monomer-monomer interface of the heterodimer (in the N-terminal domain of the β monomer), and consists of several highly conserved hydrophobic amino acids (Leu240, Leu250, Leu253 and Phe266) with a few hydrophilic residues (Thr237 and Asn256). Furthermore, the binding site contains some amino acids that have been identified as BzC resistance mutations in some fungal species (Tyr50, Gln134, Thr165 and Met257) [21].

3.2. Molecular docking

The BzC were docked into the β-tubulin model using AutoDock 4.2 in order to suggest the binding mode in the proposed binding site. For this purpose, we selected from Table 2 the lowest energy conformation of each compound from the four different groups. Fig. 3 shows the proposed binding models for these binding energies. Notably it should be emphasized that there is no experimental binding affinity that can be compared directly with the calculated binding energy. In general terms, a *cis* conformation in the carbamate and a 1,5 tautomerism in the benzimidazole favor the formation of hydrogen bonds between the Glu198 and the hydrogen in the benzimidazole and that in the carbamate group. In fact, these interactions were identified as being mainly responsible for the low binding energy calculated for the BzC with these conformations. Interestingly, the *cis* conformation also

```
1    MREIVHIQAGQCGNQIGAKFWEVISDEHGIDPTGSYHGDSDLQLERINVYYNEATGNKYV    60    3N2G:D
1    MREIVHLQAGQCGNQIGAKFWEVISDEHGIDQSGAYHGDSELQLERINVYYNEASGGKYV    60    T.spiralis_EFV50889
     *****:********************** :*:*****:***********:*  ***

61   PRAILVDLEPGTMDSVRSGPFGQIFRPDNFVFGQSGAGNNWAKGHYTEGAELVDSVLDVV   120    3N2G:D
61   PRAILVDLEPGTMDSVRAGPFGALFRPDNFIFGQSGAGNNWAKGHYTEGAELVDSVLDVV   120    T.spiralis_EFV50889
     *****************:**** :******:*****************************

121  RKESESCDCLQGFQLTHSLGGGTGSGMGTLLISKIREEYPDRIMNTFSVMPSPKVSDTVV   180    3N2G:D
121  RKESESCDCLQGFQLTHSLGGGTGSGMGTLLISKIREEYPDRIMTTFSVVPSPKVSDTVV   180    T.spiralis_EFV50889
     ******************************************.****:***********

181  EPYNATLSVHQLVENTDETYSIDNEALYDICFRTLKLTTPTYGDLNHLVSATMSGVTTCL   240    3N2G:D
181  EPYNATLSVHQLVENTDETFCIDNEALYDICFRTLKLVNPTYGDLNHLVSATMSGVTTCL   240    T.spiralis_EFV50889
     *******************. *****************..*******************

241  RFPGQLNADLRKLAVNMVPFPRLHFFMPGFAPLTSRGSQQYRALTVPELTQQMFDSKNMM   300    3N2G:D
241  RFPGQLNADLRKLAVNMVPFPRLHFFMPGFAPLTSRGSQGYRALTVPELTQQMFDAKNMM   300    T.spiralis_EFV50889
     ***************************************.*************** .****

301  AACDPRHGRYLTVAAVFRGRMSMKEVDEQMLNVQNKNSSYFVEWIPNNVKTAVCDIPPRG   360    3N2G:D
301  AACDPRHGRYLTVAAIFRGRMSMKEVDEQMLNVQNKNSAYFVEWIPNNVKTAVCDIPPRG   360    T.spiralis_EFV50889
     ***************:*********************:*********************

361  LKMSATFIGNSTAIQELFKRISEQFTAMFRRKAFLHWYTGEGMDEMEFTEAESNMNDLVS   420    3N2G:D
361  LKMSATFIGNSTAIQELFKRISEQFTAMFRRKAFLHWYTGEGMDEMEFTEAESNMNDLVS   420    T.spiralis_EFV50889
     ************************************************************

421  EYQQYQDA    428    3N2G:D
421  EYQQYQEA    428    T.spiralis_EFV50889
     ******:*
```

Fig. 1. Alignment of *O. aries* (PDB ID: 3N2G_D) and *T. spiralis* β–tubulin partial sequences used for the homology model.

enables the possible formation of another hydrogen bond between the oxygen in the carbamate and the Thr165. This interaction stands out because other susceptible species of nematodes also present hydrogen bond donors at position 165 [e.g. *Ascaris lumbricoides* [44], *Trichiuris trichiura* [45], *Brugia malayi* [20]]. It is worth noticing that the *trans* conformation in the carbamate may also form a weaker hydrogen bond with the Thr165, thus suggesting that either the *cis* or *trans* conformation can interact with amino acids at either position.

One interesting aspect of this model is that it highlights the importance of the substitution in BzC. For example, LBZ exhibits the lowest calculated docking binding energy (−9.41 kcal/mol), whereas CBZ has the highest (−7.05 kcal/mol); the structural difference between LBZ and CBZ is the substitution at position 5 in the benzimidazole nucleus ring. It was observed that the presence of a carbonyl group or a sulfoxide group at position 5 of the benzimidazole nucleus ring enables a hydrogen bond to be formed with the Cys239, as can be seen in LBZ, MBZ, NZ, ABZSO and FBZSO. This interaction helps fix the ligand inside the binding site at the same time that the distance between the carbonyl group of the carbamate and the Thr165 is reduced, thus favoring the formation of the hydrogen bond. Curiously, the ether and thioether groups in the ABZ, FBZ and OBZ can also form this hydrogen bonding. However, the hydrogen bonds formed by these groups are not usually as strong as those formed by a carbonyl or a sulfoxide group, a fact that is reflected in the calculated binding energy [46]. This result is in total agreement with the experimental information previously reported; this shows that the metabolites ABZSO and FBZSO are responsible for the antiparasitic effect rather than the parent compounds ABZ and FBZ. However, there is less probability that the enantiomer (−) binds to the binding site, since it has been reported that is the main substrate for the production of the inactive sulfone [47,48].

3.2.1. Comparison of colchicine and the model binding sites

The docked BzC partially overlap the colchicine-binding site. This is not a surprising result, and in fact, the competitive inhibition between BzC (e.g. MBZ, NZ, OBZ, FBZ) and colchicine has been reported before [8,25,28]. Fig. 4 shows the superposition of our model with the *Bos taurus* tubulin heterodimer co-crystallized with colchicine (PDB ID: 1SA0_C/D). This comparison provides insights into the similarity of the binding sites of the BzC and colchicine. As can be seen in Fig. 4, colchicine overlaps part of the benzimidazole nucleus ring and the substituent at position 5. This suggests that colchicine and the BzC may have the same mechanism of action, i.e., both may act by inducing a conformational change in the T7 loop of the β monomer, thus reducing the interaction with α monomer and promoting the generation of the curved conformation of the

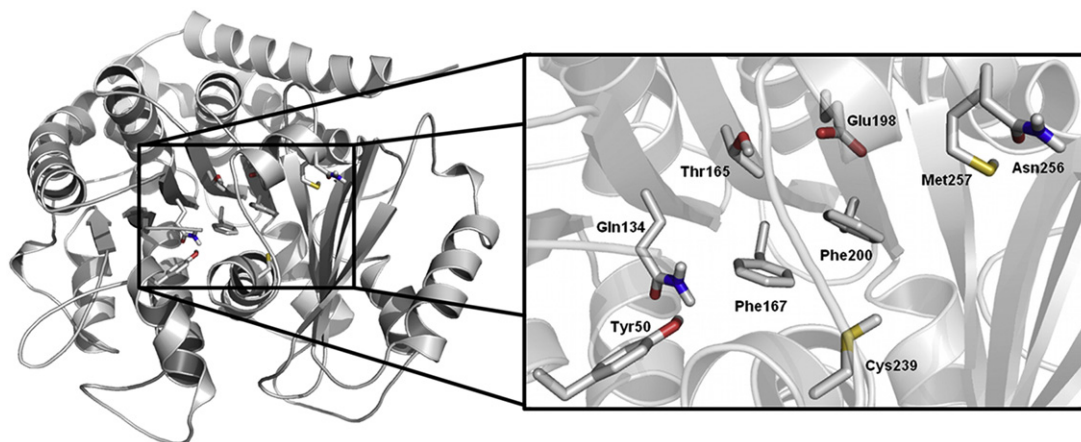**Fig. 2.** Three-dimensional representation of the model obtained for the β-tubulin of *T. spiralis*. Amino acids associated with BzC resistance are highlighted.

Table 2
Binding energies and cluster sizes of BzC in the model of β-tubulin calculated with AutoDock 4.2.

Compound	cis-1,5		trans-1,5		cis-1,6		trans-1,6	
	ΔG_{bind} (kcal/mol)	Cluster size	ΔG_{bind} (kcal/mol)	Cluster size	ΔG_{bind} (kcal/mol)	Cluster size	ΔG_{bind} (kcal/mol)	Cluster size
CBZ	−7.05[a]	9	−6.86	5	–	–	–	–
ABZ	−7.70[a]	11	−7.41	11	−7.44	6	−7.45	4
(+) ABZSO	−7.90[a]	7	−7.76	7	−7.84	5	−7.84	4
(−) ABZSO	−7.70	2	−7.47	4	−8.03[a]	9	−7.98	13
MBZ	−8.73	7	−9.08[a]	18	−8.88	12	−8.65	2
FBZ	−8.76[a]	8	−8.63	9	−8.69	12	−8.58	15
(+) FBZSO	−9.02[a]	5	−8.63	4	−8.90	2	−8.81	11
(−) FBZSO	−8.96	4	−8.90	6	−9.15[a]	13	−9.01	11
OBZ	−7.41[a]	14	−6.98	5	−6.92	7	−6.93	4
PBZ	−7.93[a]	14	−7.74	14	−7.41	1	−7.25	12
LBZ	−9.41[a]	6	−9.29	10	−8.34	3	−8.31	11
NZ	−8.83	10	−8.95[a]	14	−8.57	10	−8.57	10

[a] Lowest energy conformation for each compound.

heterodimeric structure (Fig. S3 of the Supplementary data) [32]. A heterodimer with this curved conformation is not capable of interacting with another heterodimer to form a protofilament and, for this reason, it favors the process of microtubule end depolymerization [32,49–51].

3.3. Molecular dynamics calculations

Molecular dynamics (MD) calculations were employed to assess the stability of the β-tubulin model and of the protein–ligand complexes. The former was carried out to evaluate the stability
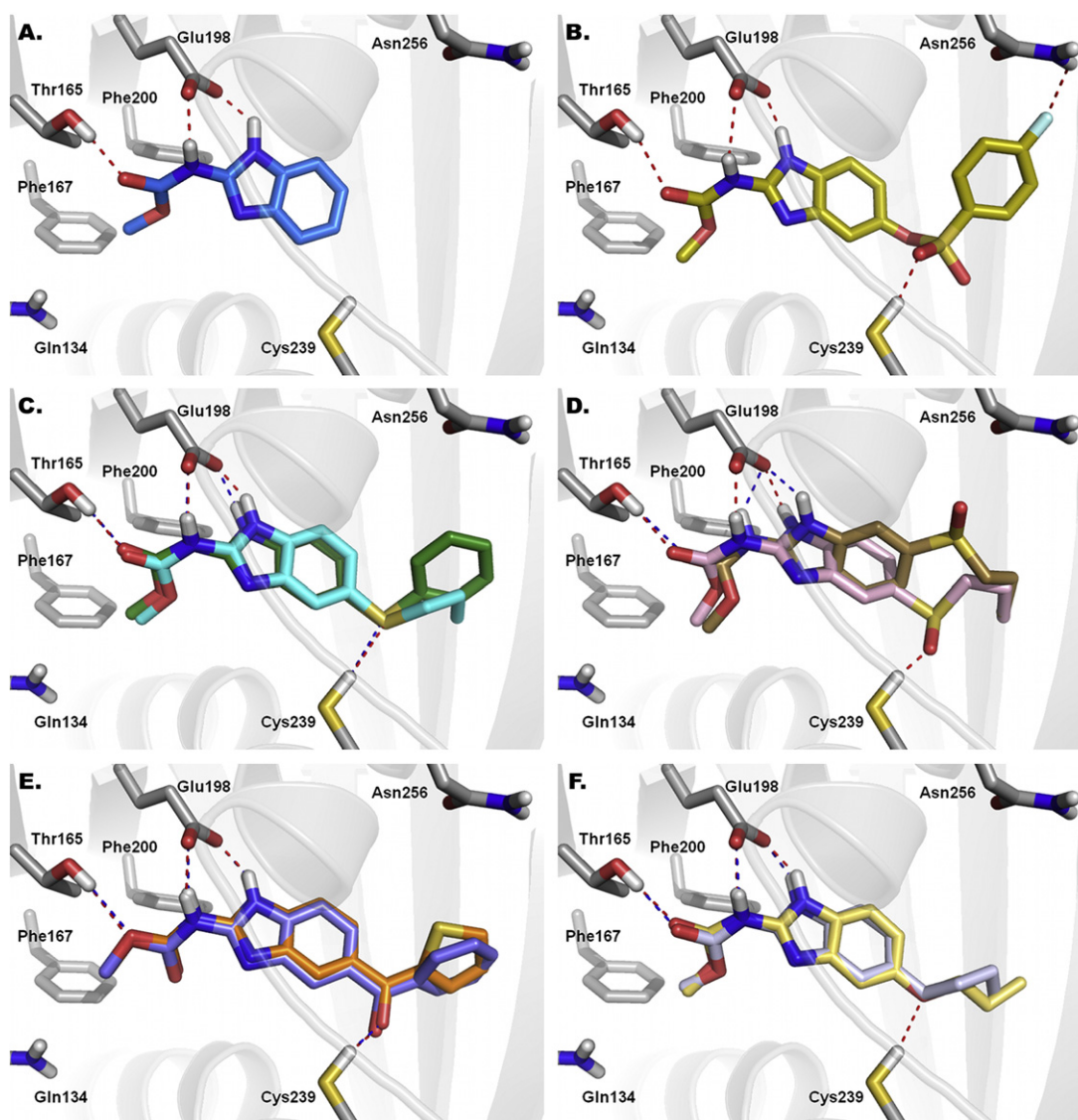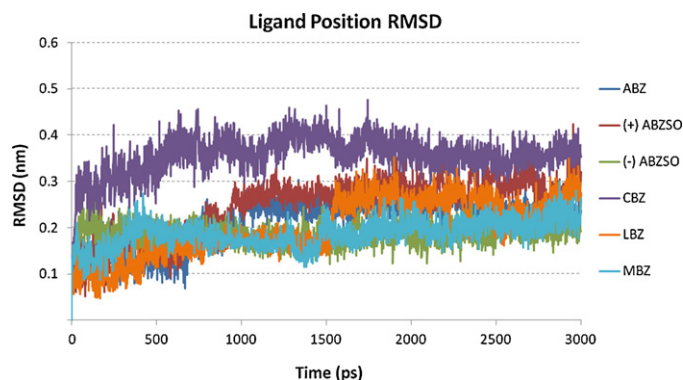

Fig. 3. Predicted binding modes of different BzC inside the proposed binding site. (A) CBZ, (B) LBZ, (C) ABZ (blue) and FBZ (green), (D) (−) ABZSO (brown) and (+) ABZSO (pink), (E) MBZ (purple) and NZ (orange), (F) OBZ (yellow) and PBZ (lilac).
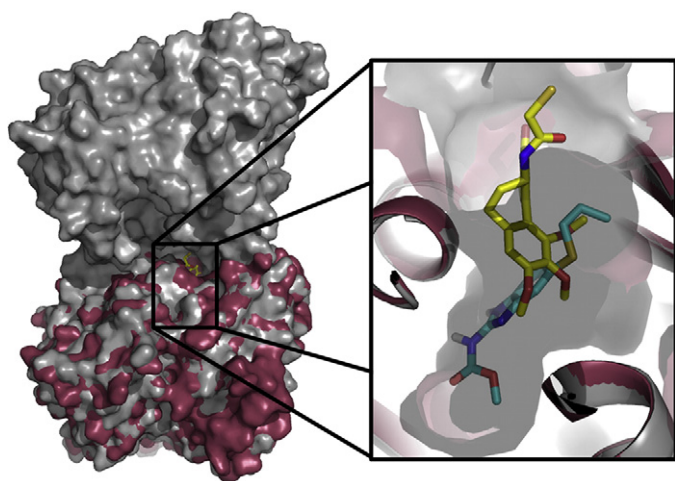
Fig. 4. Overlapped binding sites of colchicine (orange) and BzC (cyan) using the *Bos taurus* β-tubulin co-crystallized with tubulin (PDB ID: 1SA0.C/D) and our model of *T. spiralis* β-tubulin, respectively. (For interpretation of the references to color in this figure legend, the reader is referred to the web version of the article.)

Fig. 5. Ligand positional RMSD of some BzC inside the binding site of β-tubulin through 3000 ps of simulation.

of the model and to equilibrate the system. To this end, we analyzed the protein backbone RMSD for 10 ns of MD simulations, in which no changes were observed, showing a RMSD value less than 0.3 nm through the simulation. In a similar way, the ligand positional RMSD was evaluated for all the protein–ligand complexes previously obtained using molecular docking. The number of hydrogen bonds and the binding free energies based on LIE method calculated with GROMACS 4.5.3 for each BzC are reported in Table 3. Fig. 5 shows that most of the BzC presented a low RMSD throughout the simulation. Particularly, the CBZ presented the highest RMSD,

followed by those that have weak hydrogen bond acceptors in the substitution at position 5 and finally, those with sulfonates or sulfoxides substituents at position 5, showing the lowest RMSD.

The analysis of these complexes also revealed that the hydrogen bonds identified by using molecular docking were present (79.5% of the time) throughout the simulation of the molecular dynamics, especially those formed between the ligand and Glu198, since the interactions with Thr165 and Cys239 are less common. Worthy of note is the fact that the amino acid Thr165 interacts 98.1% of the time of the simulation with the amino acid Glu198. On the other hand, the Cys239 side chain flips out, moving away from the ligand and causing the hydrogen bond to disappear, except for those compounds that showed a favored coupling interaction with this amino acid from the beginning (e.g. carbonyl and sulfonate). What is more, we also identified the formation of a new hydrogen bond between the methyl carbamate group and the Gln134, which is buried inside the binding site. Fig. 6 shows that this interaction favors the

Table 3
Estimate binding free energies calculated by LIE method and hydrogen bonds of the protein–ligand complexes during molecular dynamics.

Compound	Energy (kJ/mol)					Hydrogen bonds	
	$(V_{LJ})_{bound}$	$(V_{LJ})_{free}$	$(V_{CL})_{bound}$	$(V_{CL})_{free}$	ΔG_{bind}	Range	Average
CBZ	−137.35	−8.02	11.77	8.69	−21.74	0–2	0
ABZ	−150.22	−3.15	−113.44	−59.04	−53.67	0–4	2
(+) ABZSO	−142.34	11.97	−82.07	−63.36	−37.12	0–4	1
(−) ABZSO	−155.17	8.58	−162.94	−109.64	−56.13	1–6	3
MBZ	−174.14	−3.49	−77.49	−52.84	−43.04	0–6	2
FBZ	−179.98	−2.88	−50.14	−44.40	−34.75	0–5	1
(+) FBZSO	−168.94	0.51	−110.05	−85.89	−42.58	0–5	2
(−) FBZSO	−166.05	−8.35	−106.69	−100.45	−31.51	0–5	2
OBZ	−150.29	2.87	−60.29	−51.59	−31.92	0–4	1
PBZ	−143.47	−3.06	−68.32	−44.46	−37.20	0–4	1
LBZ	−202.67	14.74	−52.67	−41.51	−44.71	0–4	1
NZ	−170.51	1.91	−34.76	−28.16	−34.34	0–4	1
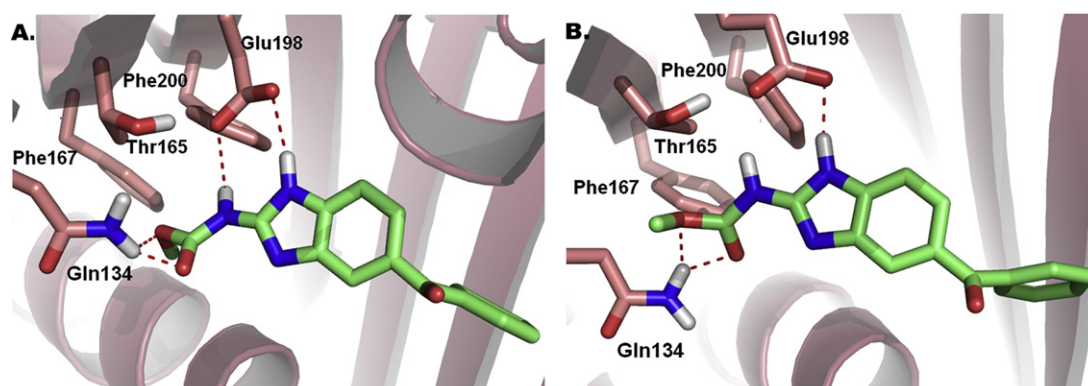
Fig. 6. Different conformations of MBZ inside the β-tubulin binding site after (a) 800 and (b) 2000 ps of simulation show a hydrogen bond interaction with Gln134.

retention of the molecule inside the binding site, internalizing the ligand into the pocket and bringing it into contact with the amino acid Glu198. Once again, CBZ was the only ligand that did not present this interaction, thus making it the least stable compound studied in this paper.

4. Conclusion

In this paper, we generated a homology model for the β-tubulin of *T. spiralis* using the crystal structure of *O. aries* β-tubulin (PDB ID: 3N2G_D) as a template. With this model, we were able to suggest a binding site for benzimidazole-2-carbamate derivatives (BzC) which was in good agreement with the experimental information previously reported. For example, it contains several amino acids associated with resistance mutations (F167Y, E198A and F200Y) and it partially overlaps the colchicine-binding site that explains the competitive inhibition between colchicine and BzC. In order to achieve a deeper insight into the proposed binding site, we conducted the molecular docking and molecular dynamics calculations of several BzC which are commonly used as antiparasitic drugs. The results suggest that BzC are stabilized inside the binding site mainly by a hydrogen bond with Thr165, Glu198, Cys239 and Gln134. Moreover, these calculations highlight the importance of a substituent with a hydrogen bond acceptor group at position 5 of the benzimidazole nucleus. With the results presented in this paper in mind, we can deduce that when the substituents at position 5 of the benzimidazole nucleus ring are sulfonates or sulfoxides, the activity will be increased (e.g. ABZSO), as compared with weak hydrogen bond acceptors, such as ether or thioether (e.g. ABZ) and will be more stable than compounds without a substitution at the same position, such as CBZ.

As a concluding remark, the identification of this binding site, which is consistent with different experimental data, could be useful for the structure-based design of new antiparasitic molecules. In fact, this model is being used by our group to study the mechanism by which mutations cause resistance against BzC in nematodes. Even though others models of β-tubulin have been published before, this is the first time that an "open conformation" of this protein is studied and this may help to capture different aspects of the protein–ligand interaction.

Acknowledgements

All molecular graphics figures were prepared with PyMOL [52].

Appendix A. Supplementary data

Supplementary data associated with this article can be found, in the online version, at http://dx.doi.org/10.1016/j.jmgm.2013.01.007.

References

[1] P.J. Hotez, Neglected infections of poverty in the United States of America, PLOS Neglected Tropical Diseases 2 (2008) e256.

[2] K.H. Downing, Structural basis for the interaction of tubulin with proteins and drugs that affect microtubule dynamics, Annual Review of Cell and Developmental Biology 16 (2000) 89–111.

[3] B.J. Fennell, J.A. Naughton, J. Barlow, G. Brennan, I. Fairweather, et al., Microtubules as antiparasitic drug targets, Expert Opinion 3 (2008) 501–518.

[4] L. Mottier, C.E. Lanusse, Bases moleculares de la resistencia a fármacos antihelmínticos, Revista de Medicina Veterinaria 82 (2001) 74–85.

[5] S.K. Katiyar, V.R. Gordon, G.L. McLaughlin, T.D. Edlind, Antiprotozoal activities of benzimidazoles and correlations with β-tubulin sequence, Antimicrobial Agents and Chemotherapy 38 (1994) 2086–2090.

[6] S. Sharma, N. Anand, Approaches to Design and Synthesis of Antiparasitic Drugs, vol. 25, Elsevier, Amsterdam, 1997, Chapter 8.

[7] G.W. Lubega, R.K. Prichard, Specific interaction of benzimidazoles anthelmintics with tubulin: high-affinity binding and benzimidazoles resistance in *Haemonchus contortus*, Molecular and Biochemical Parasitology 38 (1990) 221–232.

[8] A. Jiménez-González, C. De Armas-Serra, A. Criado-Fornelio, N. Casado Escribano, F. Rodríguez-Caabeiro, et al., Preliminary characterization and interaction of tubulin from *Trichinella spiralis* larvae with benzimidazole derivatives, Veterinary Parasitology 39 (1991) 89–99.

[9] M. Borgers, S. De Nollin, M. De Brabander, D. Thienpont, Influence of the anthelmintic mebendazole on microtubules and intracellular organelle movement in nematode intestinal cells, American Journal of Veterinary Research 36 (1975) 1153–1166.

[10] E. Lacey, K.L. Snowdon, G.K. Eagleson, E.F. Smith, Further investigations of the primary mechanism of benzimidazole resistance in *Haemonchus contortus*, International Journal for Parasitology 17 (1987) 1421–1429.

[11] E. Lacey, J.H. Gill, Biochemistry of benzimidazole resistance, Acta Tropica 56 (1994) 245–262.

[12] B. Wallner, A. Elofsson, All are not equal: a benchmark of different homology modeling programs, Protein Science 14 (2005) 1315–1327.

[13] C.N. Cavasotto, Homology models in docking and high-throughput docking, Current Topics in Medicinal Chemistry 11 (2011) 1528–1534.

[14] R.N. Beech, P. Skuce, D.J. Bartley, R.J. Martin, R.K. Prichard, et al., Anthelmintic resistance: markers for resistance or susceptibility? Parasitology 138 (2010) 160–174.

[15] M. Ghisi, R. Kaminsky, P. Mäser, Phenotyping and genotyping of *Haemonchus contortus* isolates reveals a new putative candidate mutation for benzimidazole resistance in nematodes, Veterinary Parasitology 144 (2007) 313–320.

[16] L. Rufener, R. Kaminsky, P. Mäser, In vitro selection of *Haemonchus contortus* for benzimidazole resistance reveals a mutation at amino acid 198 of β-tubulin, Molecular and Biochemical Parasitology 168 (2009) 120–122.

[17] M.S.G. Kwa, J.G. Veenstra, M.H. Roos, Benzimidazole resistance in *Haemonchus contortus* is correlated with a conserved mutation at amino acid 200 in β-tubulin isotype 1, Molecular and Biochemical Parasitology 63 (1994) 299–303.

[18] P. Shayan, A. Eslami, H. Borji, Innovative restriction site created PCR-RFLP for detection of benzimidazole resistance in *Teladorsagia circumcincta*, Parasitology Research 100 (2006) 1063–1068.

[19] A. Diawara, L.J. Drake, R.R. Suswillo, J. Kihara, D.A.P. Bundy, et al., Assays to detect β-tubulin codon 200 polymorphism in *Trichuris trichiura* and *Ascaris lumbricoides*, PLOS Neglected Tropical Diseases 3 (2009) e397.

[20] A.E. Schwab, D.A. Boakye, D. Kyelem, R.K. Prichard, Detection of benzimidazole resistance-associated mutations in the filarial nematode *Wuchereria bancrofti* and evidence for selection by albendazole and ivermectin combination treatment, The American Journal of Tropical Medicine and Hygiene 73 (2005) 234–238.

[21] M.W. Robinson, N. McFerran, A. Trudgett, L. Hoey, I. Fairweather, A possible model of benzimidazole binding to β-tubulin disclosed by invoking an interdomain movement, Journal of Molecular Graphics and Modelling 23 (2004) 275–284.

[22] F.L. Henriquez, P.R. Ingram, S.P. Muench, D.W. Rice, C.W. Roberts, Molecular basis for resistance of *Acanthamoeba* tubulins to all major classes of antitubulin compounds, Antimicrobial Agents and Chemotherapy 52 (2007) 1133–1135.

[23] E. Chambers, L.A. Ryan, E.M. Hoey, A. Trudgett, N.V. McFerran, et al., Liver fluke β-tubulin isotype 2 binds albendazole and is thus a probable target of this drug, Parasitology Research 107 (2010) 1257–1264.

[24] O.P. Sharma, A. Pan, S.L. Hoti, A. Jadhav, M. Kannan, et al., Modeling docking, simulation, and inhibitory activity of the benzimidazole analogue against β-tubulin protein from *Brugia malayi* for treating lymphatic filariasis, Medicinal Chemistry Research 21 (2011) 2415–2427.

[25] P.A. Friedman, E.G. Platzer, Interaction of anthelmintic benzimidazole derivatives with bovine brain tubulin, Biochimica et Biophysica Acta 544 (1978) 605–614.

[26] J.P. Laclette, G. Guerra, C. Zetina, Inhibition of tubulin polymerization by mebendazole, Biochemical and Biophysical Research Communications 92 (1980) 417–423.

[27] G.J. Russell, J.H. Gill, E. Lacey, Binding of [³H]benzimidazole carbamatos to mammalian brain tubulin and the mechanism of selective toxicity of the benzimidazole anthelmintics, Biochemical Pharmacology 43 (1992) 1095–1100.

[28] S.K. Tahir, P. Kovar, S.H. Rosenberg, S.C. Ng, Rapid colchicine competition-binding scintillation proximity assay using biotin-labeled tubulin, Biotechniques 29 (2000) 156–160.

[29] T.L. Nguyen, C. McGrath, A.R. Hermone, J.C. Burnett, D.W. Zaharevitz, et al., A common pharmacophore for a diverse set of colchicine site inhibitors using a structure-based approach, Journal of Medicinal Chemistry 48 (2005) 6107–6116.

[30] M. Mitreva, D.P. Jasmer, D.S. Zarlenga, Z. Wang, S. Abubucker, et al., The draft genome of the parasitic nematode *Trichinella spiralis*, Nature Genetics 43 (2011) 228–235.

[31] A. Roy, A. Kucukural, Y. Zhang, I-TASSER: a unified platform for automated protein structure and function prediction, Nature Protocols 5 (2010) 725–738.

[32] P. Barbier, A. Dorleans, F. Devred, L. Sanz, D. Allegro, et al., Stathmin and interfacial microtubule inhibitors recognize a naturally curved conformation of tubulin dimers, Journal of Biological Chemistry 285 (2010) 31672–31681.

[33] A. Fiser, R.K. Do, A. Sali, Modeling of loops in protein structures, Protein Science 9 (2000) 1753–1773.

[34] R.A. Laskowski, M.W. MacArthur, D.S. Moss, J.M. Thornton, PROCHECK: a program to check the stereochemical quality of protein structures, Journal of Applied Crystallography 26 (1993) 283–291.

[35] D. Van Der Spoel, E. Lindahl, B. Hess, G. Groenhof, A.E. Mark, et al., GROMACS: fast, flexible, and free, Journal of Computational Chemistry 26 (2005) 1701–1718.

[36] M.F. Sanner, Python: a programming language for software integration and development, Journal of Molecular Graphics and Modelling 17 (1999) 57–61.

[37] A.W. Schüttelkopf, D.M.F., V.A.N. Aalten, PRODRG–a tool for highthroughput crystallography of protein–ligand complexes, Acta Crystallographica 60 (2004) 1355–1363.

[38] W.F. van Gunsteren, S.R., Billeter, A.A., Eising, P.H. Hünenberger, P. Krüger, et al. Biomolecular Simulation: The GROMOS96 Manual and User Guide, Vdf Hochschulverlag AG an der ETH Zürich, Zürich, Switzerland, 1996, pp. 1–1042.

[39] T. Darden, D. York, L. Pedersen, Particle mesh Ewald: an Nlog(N) method for Ewald sums in large systems, Journal of Chemical Physics 98 (1993) 10089.

[40] J. Aqvist, C. Medina, J.E. Samuelsson, A new method for predicting binding affinity in computer-aided drug design, Protein Engineering 7 (1994) 385–391.

[41] A. Punkvang, P. Saparpakorn, S. Hannongbua, P. Wolschann, A. Beyer, et al., Investigating the structural basis of arylamides to improve potency against *M. tuberculosis* strain through molecular dynamics simulations, European Journal of Medical Chemistry 45 (2010) 5585–5593.

[42] A. Silvestre, J. Cabaret, Mutation in position 167 of isotype 1 β-tubulin gene of *Trichostrongylid* nematodes: role in benzimidazole resistance? Molecular and Biochemical Parasitology 120 (2002) 297–300.

[43] P. Benkert, M. Kunzli, T. Schwede, QMEAN server for protein model quality estimation, Nucleic Acids Research 37 (2009) W4–W510.

[44] J. Wang, B. Czech, A. Crunk, A. Wallace, M. Mitreva, et al., Deep small RNA sequencing from the nematode *Ascaris* reveals conservation, functional diversification, and novel developmental profiles, Genome Research 21 (2011) 1462–1477.

[45] A.B. Bennett, G.C. Barker, D.A.P. Bundy, A beta-tubulin gene from *Trichuris trichiura*, Molecular and Biochemical Parasitology 103 (1999) 111–116.

[46] C. Laurence, M. Berthelot, Observations on the strength of hydrogen bonding, Perspectives in Drug Discovery and Design 18 (2000) 39–60.

[47] L.I. Álvarez, F.A. Imperiale, S.F. Sánchez, G.A. Murno, C.E. Lanusse, Uptake of albendazole and albendazole sulphoxide by *Haemonchus contortus* and *Fasciola hepatica* in sheep, Veterinary Parasitology 94 (2000) 75–89.

[48] B.P.S. Capece, G.L. Virkel, C.E. Lanusse, Enantiomeric behaviour of albendazole and fenbendazole sulfoxides in domestic animals: pharmacological implications, The Veterinary Journal 181 (2009) 241–250.

[49] E. Nogales, Structure insights into microtubule function, Annual Review of Biochemistry 69 (2000) 277–302.

[50] A. Dorléans, B. Gigant, R.B.G. Ravelli, P. Mailliet, V. Mikol, et al., Variations in the colchicine-binding domain provide insight into the structural switch of tubulin, Proceedings of the National Academy of Sciences of the United States of America 106 (2009) 13775–13779.

[51] A. Nawrotek, M. Knossow, B. Gigant, The determinants that govern microtubule assembly from the atomic structure of GTP-tubulin, Journal of Molecular Biology 412 (2011) 35–42.

[52] W.L. DeLano, The PyMOL Molecular Graphics System, DeLano Scientific LLC, Palo Alto, CA, 2007.